

Model Precast Concrete Beam-to-Column Connections Subject to Cyclic Loading



Geraldine S. Cheok
Research Structural Engineer
Building and Fire Research
Laboratory
National Institute of
Standards and Technology
Gaithersburg, Maryland



H. S. Lew, Ph.D.
Chief
Building and Fire Research
Laboratory
National Institute of
Standards and Technology
Gaithersburg, Maryland

Experimental results of eight 1/8-scale model precast concrete beam-to-column connections are presented. The test specimens consisted of interior connections designed in accordance with the 1985 Uniform Building Code provisions for Seismic Zones 2 and 4. These tests constitute the second and third phases of a multi-year test program being conducted at the National Institute of Standards and Technology. The objective of the test program is to develop guidelines for an economical precast beam-to-column connection for regions of high seismicity. Variables considered in the research program include location of the post-tensioning steel, the use of post-tensioning bars vs. prestressing strands and fully bonded vs. partially bonded strands. Specimens were subjected to reversed cyclic loading according to a prescribed displacement history. Comparisons were made between the behavior of precast concrete specimens and the monolithic specimens tested previously in Phase I. These comparisons were based on connection strength, ductility and energy dissipation characteristics. Comparison of results with the monolithic test specimens indicates that the post-tensioned precast concrete specimens had comparable connection strengths, higher ultimate displacement ductilities and total energy dissipation to failure, but lower energy dissipation per cycle.

A study of the behavior of $\frac{1}{2}$ -scale model precast concrete beam-to-column connections subject to cyclic inelastic loading was initiated at the National Institute of Standards and Technology (NIST) in 1987. The objective of the experimental program is to develop recommended guidelines for the design of an economical precast concrete beam-to-column connection, that provides for rapid field assembly without the use of corbels, for regions of high seismicity. These connections were designed in accordance with the provisions of the 1985 Uniform Building Code (UBC) for Seismic Zones 2 and 4.

TEST PROGRAM

The test program consists of four phases. Phase I was an exploratory phase in which four monolithic specimens and two precast concrete specimens were tested. Test results of the monolithic specimens served as references for the precast concrete tests. The results from the precast tests were used to determine the viability of the connection details.

Phase II of the program involved testing six precast concrete specimens. As a result of the low energy dissipation observed for the precast concrete specimens in Phase I, several methods of increasing the energy dissipation of the precast concrete connection were explored.

Because of a lack of stiffness in the precast specimens in the later stages of the tests upon load reversal, the use of partially bonded tendons was studied in Phase III. Phase IV, currently underway, involves the study of using conventional mild reinforcing steel in conjunction with a post-tensioned precast connection.

The results of Phases II and III of the NIST test program are summarized in this paper. Results from Phase I and Phase II were reported by Cheok and Lew in Refs. 2, 3 and 4.

Test Procedure

Boundary conditions for the test specimens are shown schematically in Fig. 1. The column bottom was pinned and the column top and beam ends were roller supported. The test setup

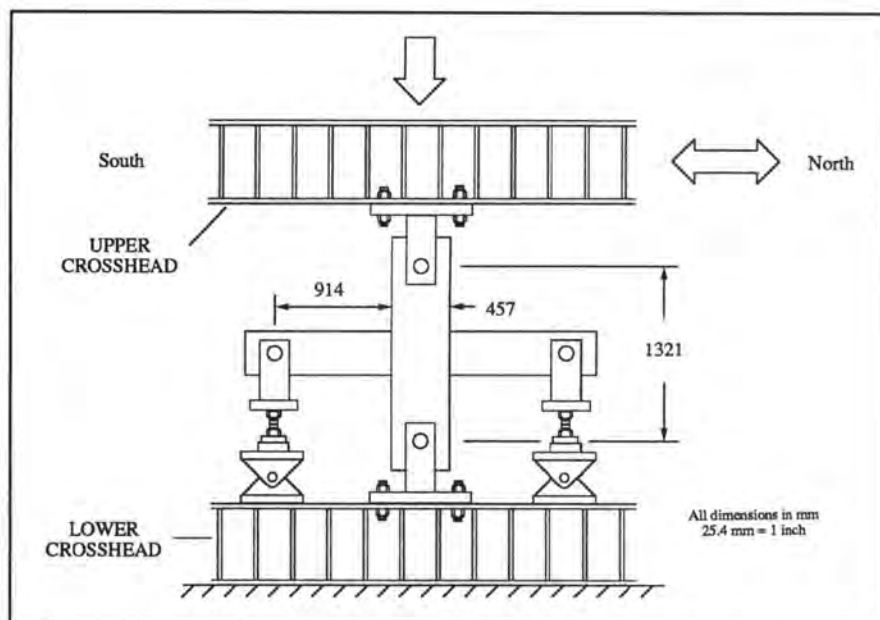


Fig. 1. Schematic of the loading and boundary conditions for the test specimens.

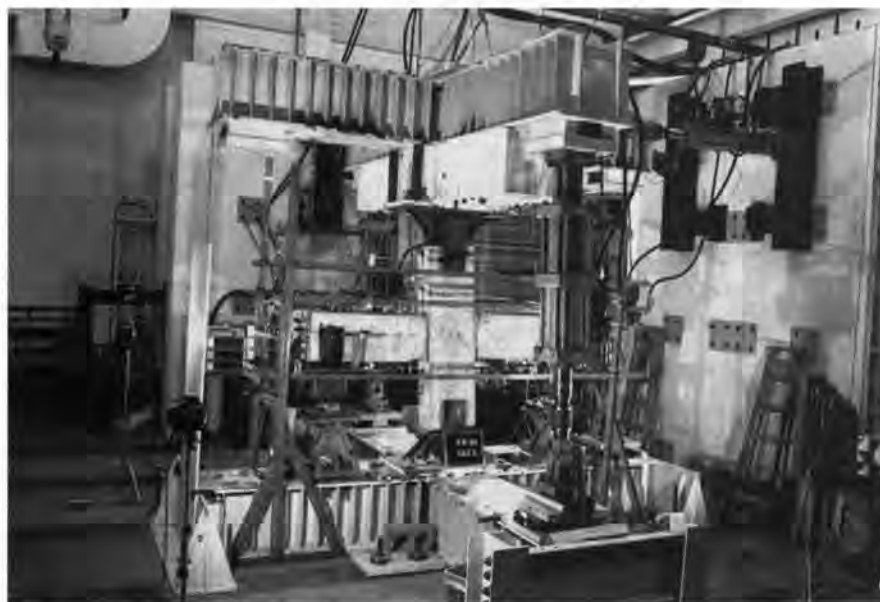


Fig. 2. Test setup and loading arrangement.

and loading arrangement are shown in Fig. 2.

An axial load equal to $0.1 f'_c A_g$ was applied to the column at the beginning of the test and maintained throughout the test. The column was then laterally loaded at the column top for the initial elastic cycle. This initial elastic cycle developed a load equal to 75 percent of the maximum strength of the monolithic beam calculated using nominal values for the material properties. The top column displacements in the forward (south) and reverse (north) directions were measured.

The "yield" displacement, Δ_y , was

defined as the average of these two displacements divided by 0.75. As defined in the previous paragraph, the yield displacement obtained for the precast concrete specimens was actually a nominal yield displacement as yielding of the post-tensioning steel did not occur in the initial elastic cycle. Henceforth, the term yield displacement should be taken to mean the nominal yield displacement.

After the initial elastic cycle, the basic loading history was two cycles each at $\pm 2\Delta_y$ and $\pm 4\Delta_y$, three cycles each at $\pm 6\Delta_y$ and $\pm 8\Delta_y$, two cycles at $\pm 10\Delta_y$, and three cycles at $\pm 12\Delta_y$.

Table 1. Specimen description.

Test phase	Specimens	Seismic zone	Type*	Post-tensioning steel†	Grouted‡	Bar distance from extreme fiber (mm)	Length of debonded post-tensioning steel (mm)
I	A-M-Z2 & B-M-Z2	2	M	—	—	—	—
I	A-M-Z4 & B-M-Z4	4	M	—	—	—	—
I	A-P-Z4 & B-P-Z4	4	P	B	F	89	—
II	A-P-Z2 & B-P-Z2	2	P	S	F	63	—
II	C-P-Z4 & D-P-Z4	4	P	B	F	135	—
II	E-P-Z4 & F-P-Z4	4	P	S	F	102	—
III	G-P-Z4 & H-P-Z4	4	P	S	P	102	1219

* M = Monolithic; P = Precast

† B = Post-tensioning bars; S = Prestressing strands

‡ F = Fully grouted; P = Partially grouted

Note: 25.4 mm = 1 in.

This loading history is similar to those used by other researchers [e.g., Bhatt and Kirk,⁵ Bull and Park,⁶ French et al.⁷]. The test was stopped whenever failure occurred.

Displacement ductility, μ , is defined as the ratio of the maximum displacement achieved in any cycle to the yield displacement. Ultimate displacement ductility, μ_u , is defined as the ratio of the maximum displacement achieved at failure to the yield displacement. Failure was considered to have occurred when the lateral force during a cycle dropped below 80 percent of the maximum lateral load that was achieved in the first cycle at $2\Delta_y$.

Strains in the beam steel and ties were measured using resistance-type strain gauges. The gauges were placed at specified locations along the beam flexural steel. In the case of the precast concrete specimens, only the mild steel reinforcing bars in the beam were instrumented (not the post-tensioning steel). In addition, the applied lateral load at the column top, the displacement of the column top, beam loads and concrete strain at various locations along the beam were measured throughout the tests.

Phases II and III Specimens

The results of the Phase I tests indicated that post-tensioned, precast concrete specimens designed using the 1985 UBC Seismic Zone 4 criteria as

design guidelines were as strong and as ductile as the monolithic Zone 4 specimens. However, compared with the monolithic specimens, the cumulative and average cyclic energy dissipated by the precast concrete specimens were 20 and 70 percent lower, respectively.

In an effort to improve the energy dissipation characteristics of the precast concrete connection, several parameters were studied in Phases II and III. One such parameter was the location of the post-tensioning steel in the beams. It was felt that the integrity of the connection would be improved if the post-tensioning steel were moved closer to the beam centroid. By doing this, the post-tensioning steel would experience less strain and would, therefore, retain its clamping force at higher drift levels.

Also, the difference in connection behavior by the use of prestressing strands instead of post-tensioning bars was examined. This variable was included in the study because prestressing strands are used more frequently in practice.

When the Phases I and II tests were conducted, concern was raised regarding the zero slope of the hysteresis loops upon load reversal that was observed in the precast concrete tests. This lack of stiffness observed in the later stages of the tests was thought to be caused by the inelastic response of the post-tensioning steel. A possible solution to this problem was to leave the strands un-

bonded through the joint region.

This concept was developed by Priestley and Tao.⁸ Briefly, the strains in the post-tensioning steel would be kept in the elastic range and the post-tensioning force would, therefore, be maintained at higher drift levels and thereby preserve the connection stiffness upon load reversal. Special interlocking spirals were provided in the beam hinge region because high compressive strains were expected in this location. A volumetric ratio of 2 percent with a maximum spiral pitch of $D/4$, where D is the spiral diameter, was used to design the confining spirals.

A summary of the specimens tested in Phases I, II and III is given in Table 1. Phase II of the test program consisted of testing three sets of specimens. The Phases II and III precast specimens were designed in a manner similar to the Phase I specimens. The required amount of post-tensioning steel was computed so that the predicted strength of the precast connection was the same as that of the monolithic connection.

Reinforcement details for the precast columns, for both Zones 2 and 4, were the same as those of the corresponding monolithic specimens. The reinforcement details for the Zone 4 precast beams were identical to those of the Phase I precast specimens except for the location of the post-tensioning steel.

Fig. 3 shows the reinforcement de-

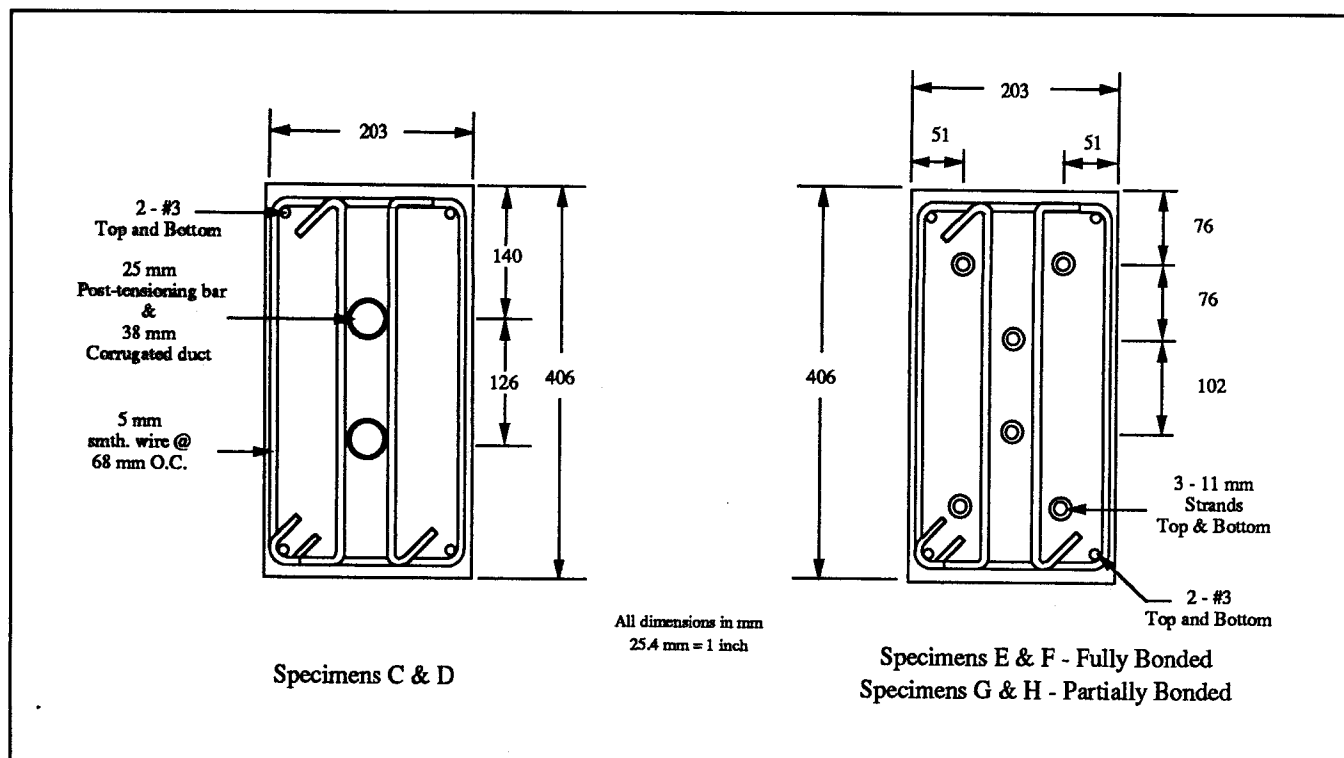


Fig. 3. Beam cross sections for Phases II and III precast concrete Zone 4 specimens.

tails for the precast Zone 4 specimens and Fig. 4 shows the reinforcement details for the Zone 2 specimens. The reinforcing bars located in the corners of the beams did not cross the joint since they were used mainly to hold the ties together. The main resistance to the applied loads was provided by the post-tensioning steel.

Material Properties

The stress-strain curves for the #3 reinforcing bars, smooth wire used in the beams and the high strength steel are shown in Figs. 5 through 12. The stress-strain curves for the smooth wire used in Specimens A-P-Z2 and B-P-Z2 and E-P-Z4 and F-P-Z4 are similar to those for Specimens G-P-Z4 and H-P-Z4.

Application of Post-Tensioning

A major concern in the use of strands was the load loss in the strand forces due to seating of the wedges. This loss was expected to be significant due to the short lengths of strands involved. A procedure which involved shimming of the chucks was followed to minimize the load loss.

When the test specimens were post-tensioned, only two load cells were

Table 2. Load cell readings after post-tensioning.

Specimen	Load Cell 1*	Load Cell 2†
E-P-Z4	0.65 F_{pu}	0.65 F_{pu}
F-P-Z4	0.65 F_{pu}	0.67 F_{pu}
G-P-Z4	0.66 $F_{pu}‡$	0.66 $F_{pu}‡$
H-P-Z4	0.68 $F_{pu}‡$	0.64 $F_{pu}‡$
A-P-Z2	0.71 $F_{pu}§$	0.67 $F_{pu}§$
B-P-Z2	0.69 $F_{pu}§$	0.70 $F_{pu}§$

* Top set of strands.

† Bottom set of strands.

‡ Average of loads from strain gauges and load cells.

§ 13 mm (0.5 in.) prestressing strands.

used — one top and one bottom for Specimens E-P-Z4 and F-P-Z4 and A-P-Z2 and B-P-Z2. Six load cells were used for Specimens G-P-Z4 and H-P-Z4. In addition to the load cells, the strands in Specimens G-P-Z4 and H-P-Z4 were instrumented with strain gauges. These gauges were located in the unbonded part of the strands.

The loads measured immediately after post-tensioning are given in Table 2. As indicated in Table 2, the loads in the individual load cells were within one standard deviation of the mean as obtained in the trial runs. The post-tensioning steel was grouted one

day after the post-tensioning operation and the time between post-tensioning and testing the specimens ranged from 2 to 4 weeks.

TEST RESULTS

Load-Displacement and Ductility

The hysteresis loops for Phases II and III specimens are shown in Figs. 13 through 20. The load and displacement in these figures represents the applied lateral force and the displacement at the column top. The hysteresis plots for the Zones 2 and 4 monolithic

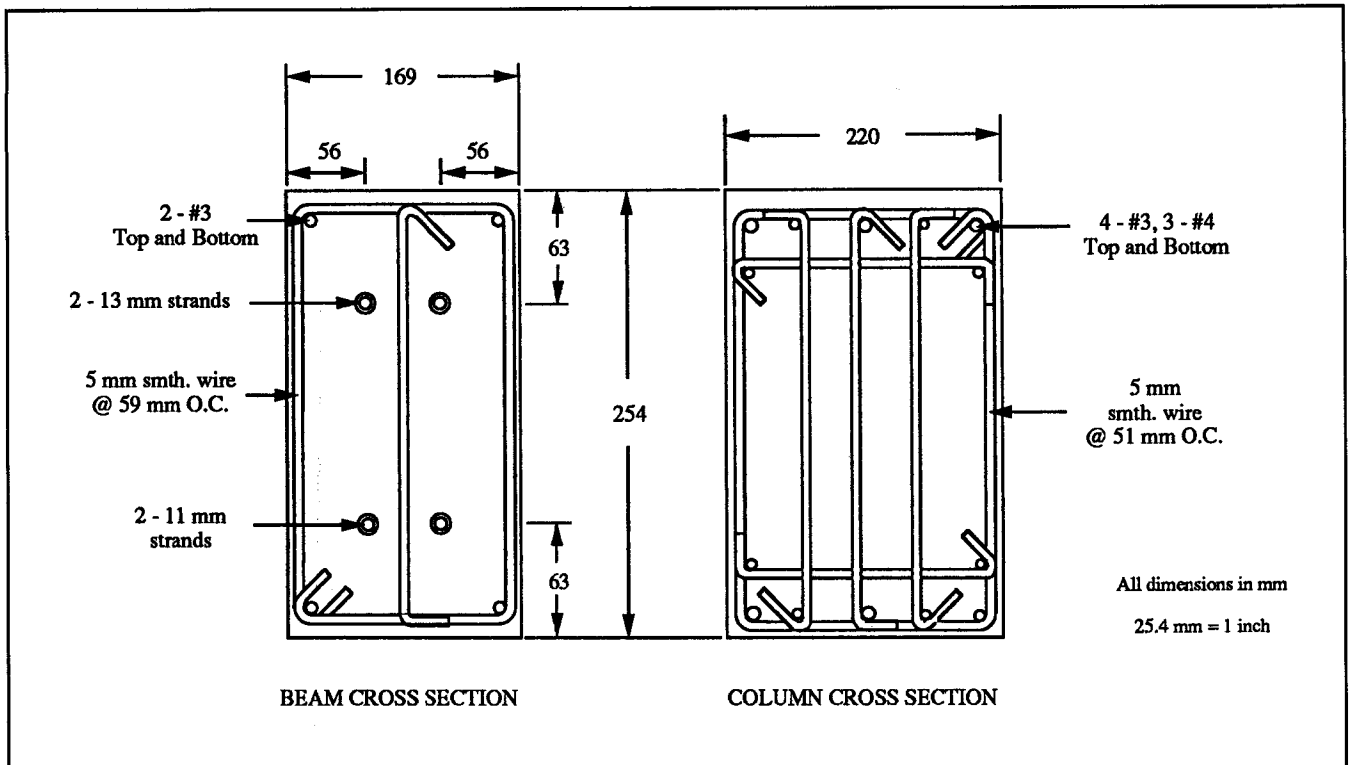


Fig. 4. Reinforcement details for Phase II precast concrete Zone 2 specimens.

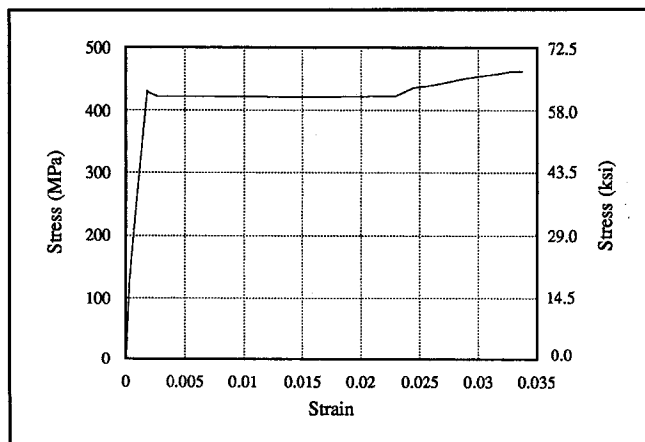


Fig. 5. Stress-strain curve for #3 reinforcing bars, Specimens A-P-Z4 to D-P-Z4, A-P-Z2 and B-P-Z2.

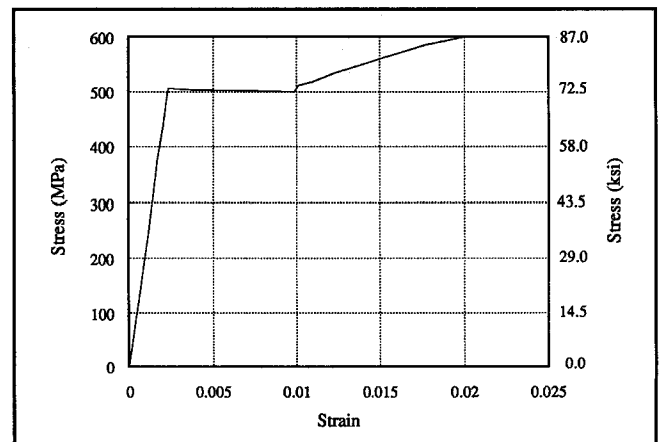


Fig. 6. Stress-strain curve for #3 reinforcing bars, all monolithic, Specimens E-P-Z4 and F-P-Z4.

specimens (from Phase I) are shown in Figs. 21 and 22, respectively, for comparison purposes.

The ductilities of the precast Zone 4 specimens, as shown in Figs. 13 through 18, are greater than that of the monolithic Zone 4 specimen, as can be seen from Fig. 22. However, the hysteresis loops for the precast concrete specimens are more severely pinched than those for the monolithic specimen. The pinched hysteresis loops probably result from the combination of the concentration of rotation at the column face due to yielding of the ten-

sons and debonding of the strands during the test which allowed some slippage to occur.

The shape of the hysteresis loops for the fully bonded precast specimens (see Figs. 15 and 16) differ from those for the partially bonded specimens shown in Figs. 17 and 18. As seen in these figures, the partially bonded specimens did not exhibit zero stiffness upon load reversal. However, the loops for the partially bonded specimens are narrower than those for the fully bonded specimens.

The experimental yield displacements and ultimate displacement ductilities for all the specimens (Phases I, II and III) are listed in Table 3. It should be noted that the yield displacements for the precast concrete specimens in Table 3 are nominal yield displacements and μ_u is based on this nominal yield displacement. Also listed in Table 3 are the initial connection stiffnesses and story drifts at failure.

Both precast Zone 2 specimens had an ultimate displacement ductility of 4, which is 50 percent less than the ductility of the corresponding monolithic specimens. The yield displacements and ultimate displacement ductilities for all the specimens (Phases I, II and III) are listed in Table 3. It should be noted that the yield displacements for the precast concrete specimens in Table 3 are nominal yield displacements and μ_u is based on this nominal yield displacement. Also listed in Table 3 are the initial connection stiffnesses and story drifts at failure.

Both precast Zone 2 specimens had an ultimate displacement ductility of 4, which is 50 percent less than the ductility of the corresponding monolithic specimens. The yield displacements and ultimate displacement ductilities for all the specimens (Phases I, II and III) are listed in Table 3. It should be noted that the yield displacements for the precast concrete specimens in Table 3 are nominal yield displacements and μ_u is based on this nominal yield displacement. Also listed in Table 3 are the initial connection stiffnesses and story drifts at failure.

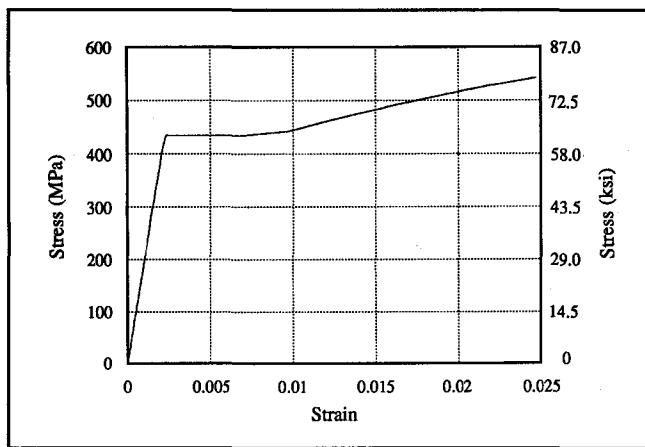


Fig. 7. Stress-strain curve for #3 reinforcing bars, Specimens G-P-Z4 and H-P-Z4.

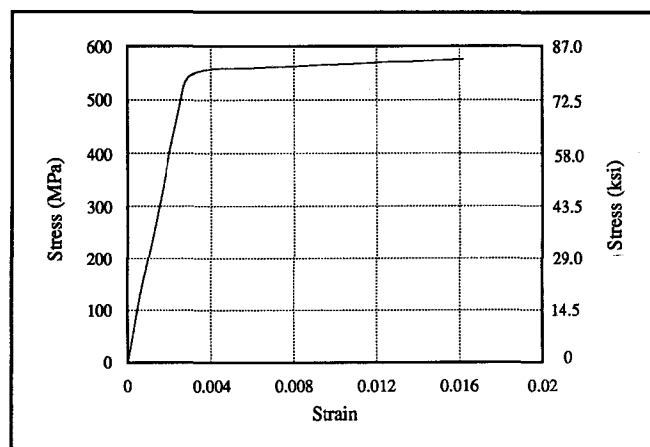


Fig. 8. Stress-strain curve for smooth wire, Specimens A-P-Z4 to D-P-Z4.

ments for the Zone 2 specimens, monolithic and precast, were approximately the same. However, due to the higher ductilities achieved by the monolithic specimens, the story drifts at failure were 65 percent greater for the monolithic specimens.

As listed in Table 3, all the Zone 4 precast specimens achieved higher ultimate displacement ductilities than those of the monolithic specimens. The displacement ductilities listed in Table 3 for Specimens G-P-Z4 and H-P-Z4 are minimum values because the

tests for these specimens were stopped prior to failure. At $\mu_u = 14$ (story drift ≈ 4 percent), the specimens did not exhibit any signs of strength degradation, and it was thought that the specimens would not fail unless the strands fractured. The expected displacement ductility of 15.6 for these specimens⁸ compares well with the experimental minimum value of 14.

The initial connection stiffnesses for the Zone 4 precast specimens were higher than those for the companion monolithic specimens. Approximate

increases in stiffness were 85 percent for precast Specimens A, B, G and H, 95 percent for precast Specimens C and D, and 135 percent for precast Specimens E and F. The fully bonded precast specimens post-tensioned with strands (Specimens E and F) were stiffer and achieved slightly higher story drifts at failure than did the specimens post-tensioned with fully bonded bars (Specimens C and D). Also, the precast specimens with fully bonded steel had slightly higher initial connection stiffnesses when the post-

Table 3. Yield displacement and ultimate displacement ductility.

Specimen designation	Concrete compressive strength, f'_c *		Experimental yield displacement		Ultimate displacement ductility, μ_u	Initial elastic connection stiffness [†]		Ultimate story drift (percent)
	MPa	(psi)	mm	(in.)		kN/m	(kips/in.)	
A-M-Z2	43.5	(6310)	9.1	(0.359)	6	7.7	(44)	4.1
B-M-Z2	41.1	(5960)	9.4	(0.371)	6	6.6	(38)	4.3
A-P-Z2	34.0	(4930)	8.5	(0.333)	4	12.4	(71)	2.6
B-P-Z2	36.4	(5280)	8.4	(0.330)	4	11.0	(63)	2.5
A-M-Z4	30.7	(4450)	6.7	(0.263)	6	21.2	(121)	3.0
B-M-Z4	32.2	(4670)	7.4	(0.293)	6	18.0	(103)	3.4
A-P-Z4	40.6	(5890)	4.1	(0.160)	10	35.7	(204)	3.1
B-P-Z4	44.5	(6450)	4.5	(0.179)	10	37.8	(216)	3.4
C-P-Z4	46.8	(6780)	5.3	(0.209)	12	31.5	(180)	4.8
D-P-Z4	44.9	(6510)	5.4	(0.213)	12	45.2	(258)	4.9
E-P-Z4	29.2	(4230)	5.7	(0.225)	12	42.2	(241)	5.2
F-P-Z4	27.7	(4020)	5.5	(0.218)	12	50.1	(286)	5.0
G-P-Z4	30.1	(4370)	3.6	(0.143)	14‡	36.1	(206)	3.9
H-P-Z4	32.2	(4680)	3.4	(0.135)	14‡	35.4	(202)	3.6

* Strengths were obtained at the time of specimen testing.

† These values are the initial elastic stiffness as obtained from the slope of the load-displacement plot for the initial excursion to $+0.75\Delta_y$.

‡ The specimens did not fail at this ductility level. Therefore, these are minimum values for the specimens.

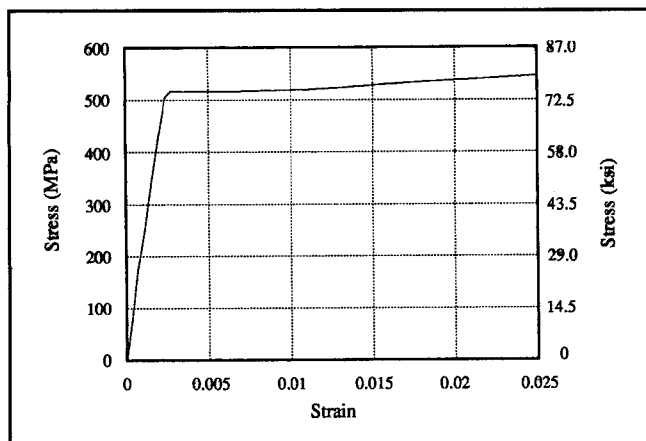


Fig. 9. Stress-strain curve for smooth wire, Specimens G-P-Z4 and H-P-Z4.

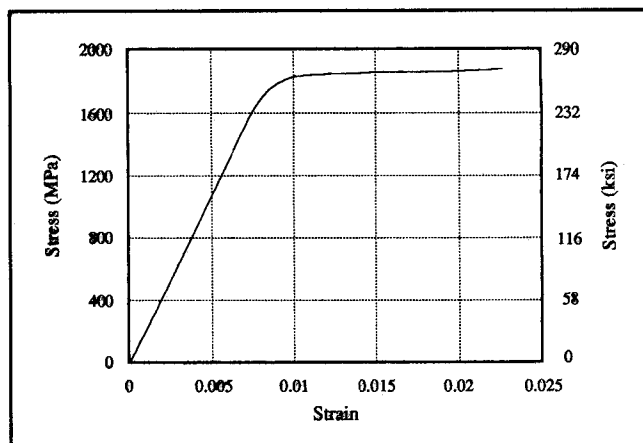


Fig. 10. Stress-strain curve for 7/16 in. (11 mm) strands, Specimens E-P-Z4 to H-P-Z4.

tioning steel was moved closer to the beam centroid.

Flexural Strength

The maximum measured and calculated moments are listed in Table 4. The calculated values were based on an ultimate concrete compressive strain of 0.003 and actual material properties. The calculated ultimate moments for the monolithic specimens had a factor of 1.25 applied to the steel yield stress to account for possible higher actual

material strengths and strain hardening. No factor for strain hardening was used to calculate the moments for the precast concrete specimens.

The moments for the partially bonded specimens were calculated based on ACI-318 Eq. (18-4)⁹ for determining the stress in the strands at nominal strength. Again, actual material properties were used. The experimental values were obtained by multiplying the peak load recorded in the beam load cell and the moment arm to the column face.

The measured maximum moments for the monolithic specimens were achieved at or close to the ultimate displacement ductility of the specimens. This was also true for precast Specimens A-P-Z2, B-P-Z2, A-P-Z4 and B-P-Z4. However, the measured maximum moments for the precast concrete specimens with the post-tensioning steel closer to the beam centroid (Specimens C-P-Z4 through F-P-Z4) were achieved earlier in the tests (at $\mu \approx 4$ whereas $\mu_u \approx 12$). The measured maximum moments for the partially bonded

Table 4. Experimental and calculated maximum moments.

Specimen designation (1)	Concrete compressive strength f'_c * (2)		Calculated maximum moment (3)		Experimental maximum moment† (4)		Avg. exp. moment Calc. max. moment (5)
	MPa	(psi)	kN-m	kip-ft	kN-m	kip-ft	
A-M-Z2	43.5	(6310)	68	50	69 & 80	51 & 59	1.10
B-M-Z2	41.1	(5960)	68	50	70 & 75	52 & 55	1.07
A-P-Z2	34.0	(4930)	46	34	52 & 54	38 & 40	1.15
B-P-Z2	36.4	(5280)	46	34	50 & 54	37 & 40	1.13
A-M-Z4	30.7	(4450)	132	97	148 & 144	109 & 106	1.11
B-M-Z4	32.2	(4670)	132	97	148 & 153	109 & 113	1.14
A-P-Z4	40.6	(5890)	155	114	176 & 186	130 & 137	1.16
B-P-Z4	44.5	(6450)	155	114	184 & 186	136 & 137	1.20
C-P-Z4	46.8	(6780)	145	107	169 & 171	125 & 126	1.17
D-P-Z4	44.9	(6510)	145	107	165 & 169	122 & 125	1.15
E-P-Z4	29.2	(4230)	111	82	138 & 136	102 & 100	1.24
F-P-Z4	27.7	(4020)	111	82	146 & 137	108 & 101	1.28
G-P-Z4	30.1	(4370)	95	70	118 & 123	87 & 91	1.27
H-P-Z4	32.2	(4680)	95	70	130 & 132	96 & 97	1.38

* Strengths were obtained at the time of specimen testing.

† Moments are at the two column faces.

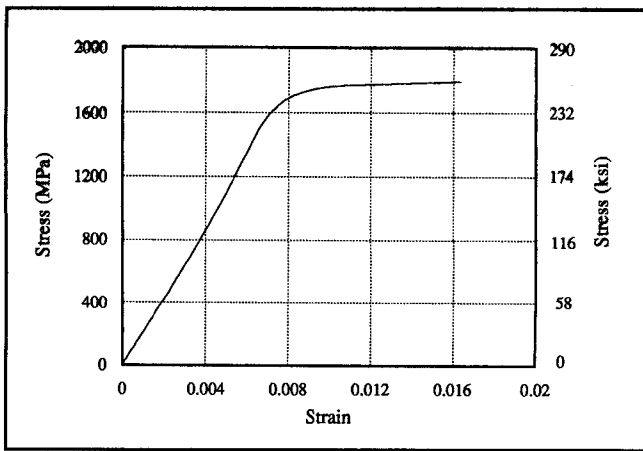


Fig. 11. Stress-strain curve for 1/2 in. (13 mm) strands, Specimens A-P-Z2 and B-P-Z2.

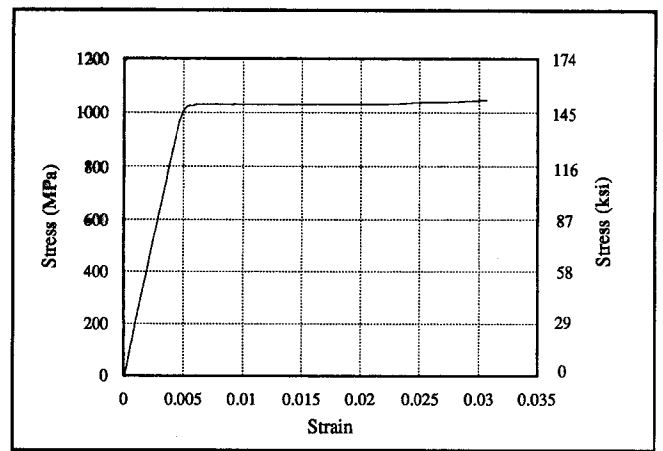


Fig. 12. Stress-strain curve for 1 in. (25 mm) Dywidag bars, Specimens A-P-Z4 to D-P-Z4.

specimens (minimum $\mu_u = 14$) were obtained at $\mu \approx 10$.

It would appear that the fully bonded precast concrete specimens with the post-tensioning steel located closer to the beam centroid debonded early in the test and behaved in a manner similar to the partially bonded specimens. Debonding of the steel in the specimens with the post-tensioning steel further away from the beam centroid may also have occurred, and the higher moments achieved in the later stages of the tests may be a result of the strain hardening of the steel.

As shown in Column 4 of Table 4, the fully bonded precast Zone 4 specimens (A-P-Z4 to F-P-Z4) were as strong as or stronger than their monolithic counterparts. When comparing

the results of Specimens A-P-Z4 and B-P-Z4 with those of Specimens C-P-Z4 and D-P-Z4, the reduction in strength caused by moving the post-tensioning bars closer to the beam centroid was approximately 8 percent. The expected reduction in connection strength (Column 3, Table 4) for these specimens was 6 percent. The ratios given in Column 5 of Table 4 indicate that the precast concrete specimens post-tensioned with strands had more "reserve" strength than those post-tensioned with high strength bars — an average of 29 percent greater than the calculated moment for the strands as opposed to 17 percent for the bars. The experimental strength of the partially bonded specimens (G-P-Z4 and H-P-Z4) was approximately 10 percent less

than that of the fully bonded specimens (E-P-Z4 and F-P-Z4).

Failure Modes

The failure mode for the precast Zone 2 specimens was beam crushing. This is different from the failure mode for the monolithic Zone 2 specimens, which failed predominantly in shear in the column joint region. The precast specimens did not sustain significant damage in the joint region. The beam-to-column opening for the precast Zone 2 specimens was approximately 5 mm (0.2 in.). This is one-fifth of the opening size for the precast Zone 4 specimens. There are insufficient data to determine if this is a result of the higher initial beam stress resulting

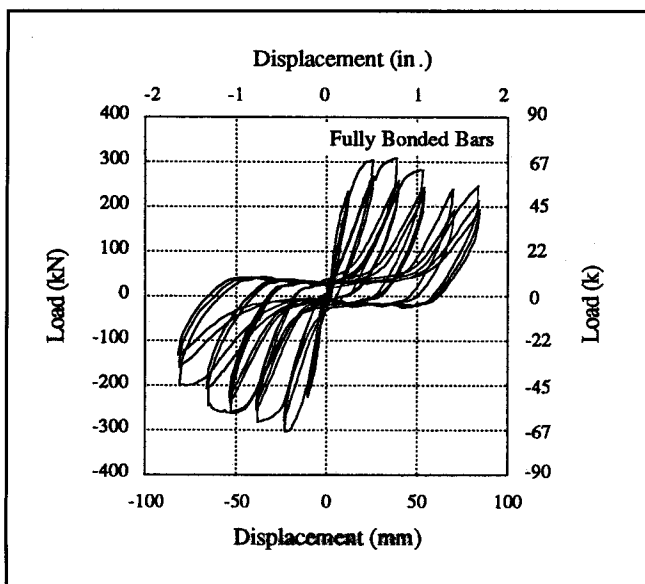


Fig. 13. Hysteresis plot for Specimen C-P-Z4.

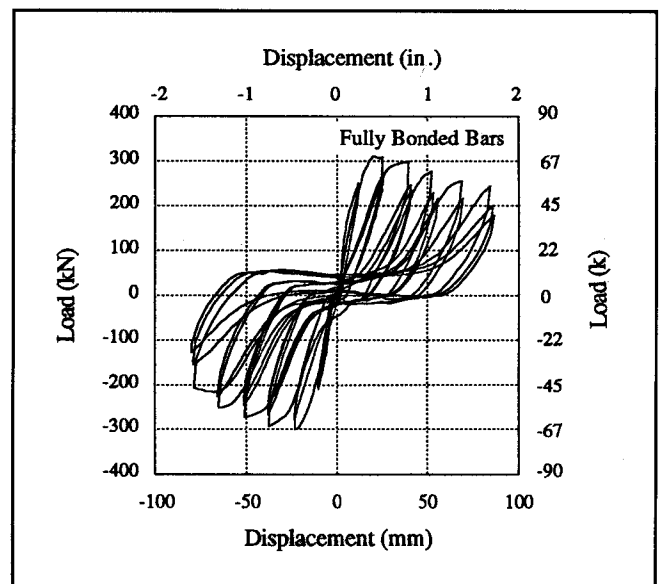


Fig. 14. Hysteresis plot for Specimen D-P-Z4.

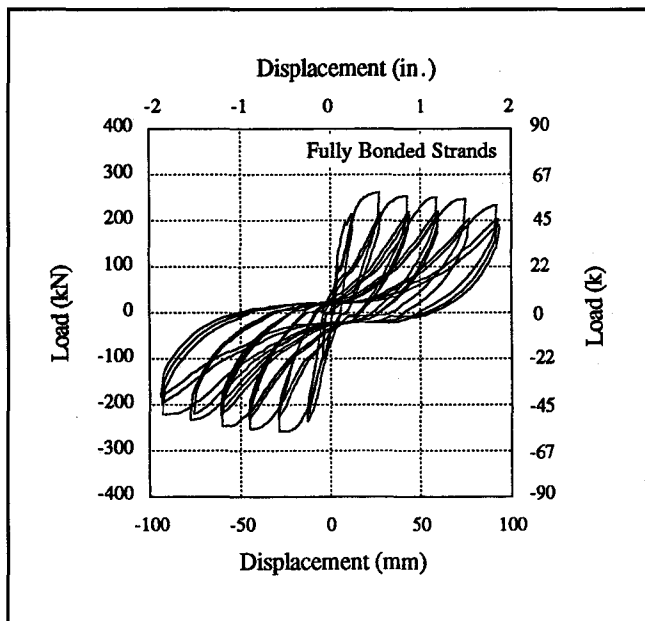


Fig. 15. Hysteresis plot for Specimen E-P-Z4.

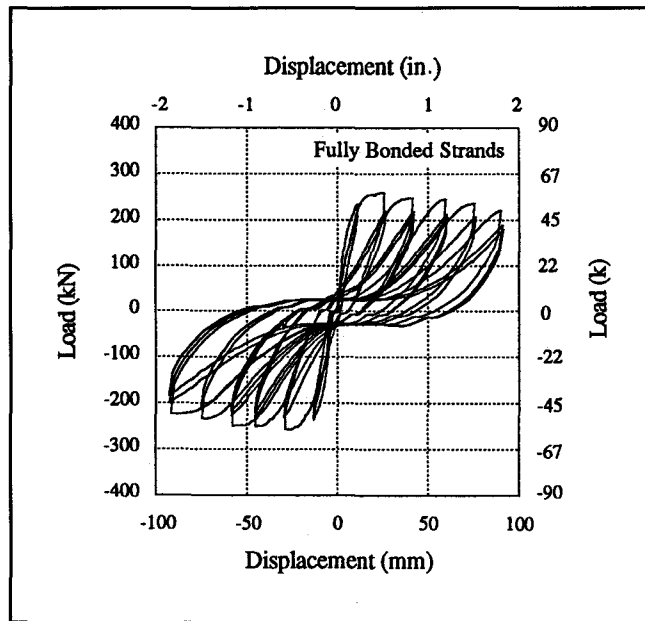


Fig. 16. Hysteresis plot for Specimen F-P-Z4.

from the post-tensioning of the Zone 2 specimens, or the result of the lower loads experienced by these specimens.

The failure modes for all the precast Zone 4 specimens were similar to those for the precast Zone 2 specimens. One of the precast Zone 4 connections after failure is shown in Fig. 23. The precast concrete beams sustained less cracking than did the beams in the monolithic specimens, and concentration of beam hinging at the column face was observed. However, more beam crushing and a wider opening between the beam and col-

umn, approximately 50 percent greater, was observed in the precast specimens which had the post-tensioning steel closer to the beam centroid.

The partially bonded precast specimens experienced more crushing of the beams than did the fully bonded specimens. However, the width of the opening between the beam and column was similar in both sets of precast concrete specimens. The column joint regions in the partially bonded precast specimens appeared to sustain the same amount of damage as the fully bonded set of precast specimens.

Energy Dissipation Characteristics

Fig. 24 shows a comparison of the energy dissipated per cycle for all the precast Zone 4 specimens. As seen in the chart, Specimens E-P-Z4 and F-P-Z4 (fully bonded strands) performed the best and Specimens G-P-Z4 and H-P-Z4 (partially bonded strands) performed the worst in terms of energy dissipated per cycle. Again, the low cyclic energy dissipated by the partially bonded specimens was due to the expected bilinear elastic behavior of these specimens.

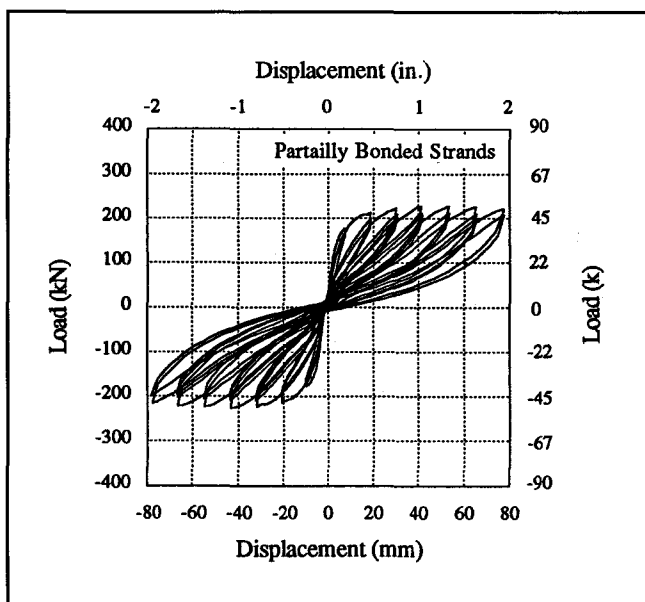


Fig. 17. Hysteresis plot for Specimen G-P-Z4.

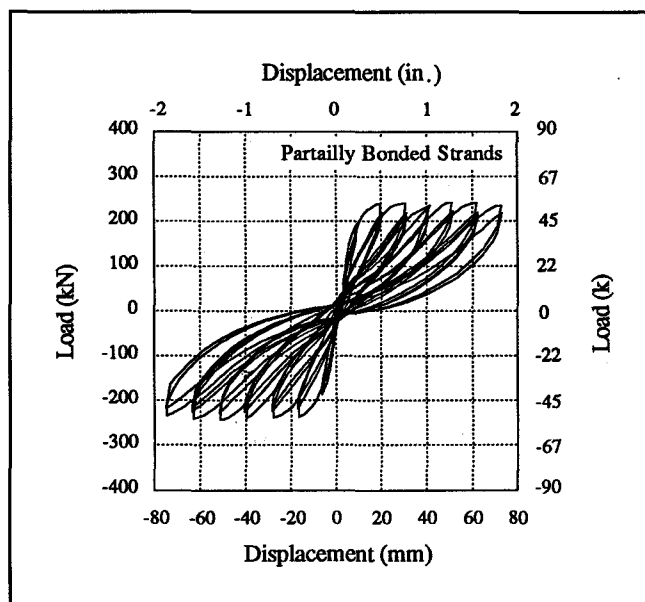


Fig. 18. Hysteresis plot for Specimen H-P-Z4.

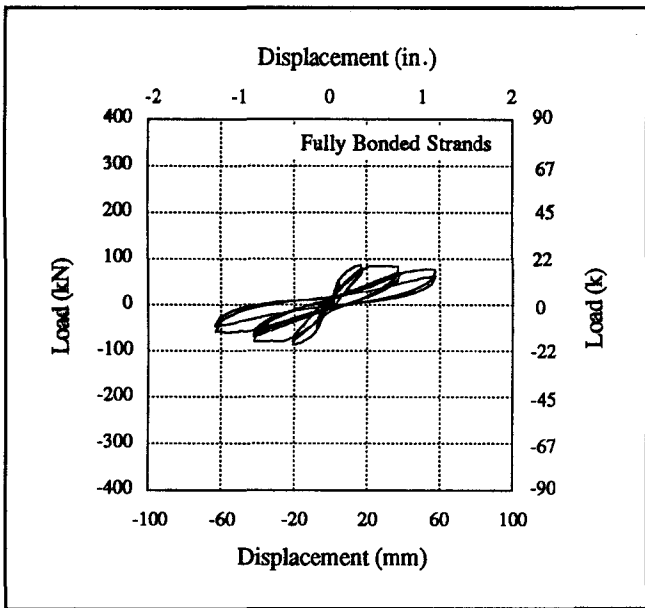


Fig. 19. Hysteresis plot for Specimen A-P-Z2.

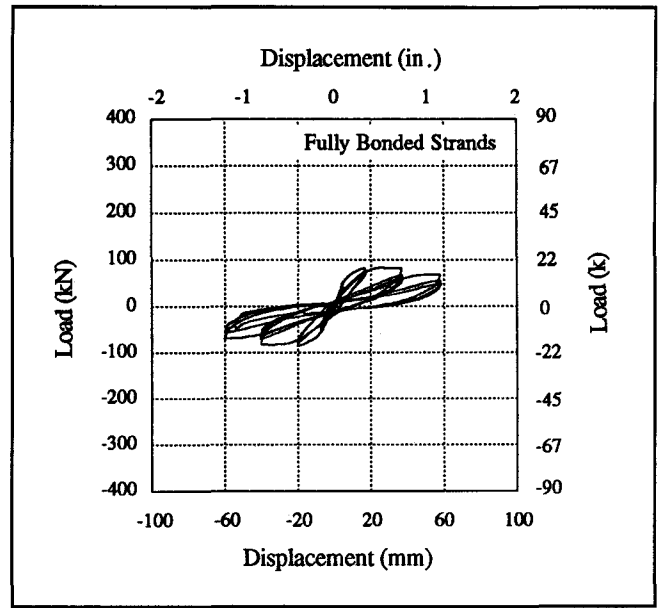


Fig. 20. Hysteresis plot for Specimen B-P-Z2.

Comparing the results of Specimens A-P-Z4 and B-P-Z4 with those of Specimens C-P-Z4 and D-P-Z4, the energy dissipated per cycle showed an average increase of 45 percent ($\sigma = 24$ percent) when the post-tensioning bars were moved closer to the beam centroid. This increase is probably due to the increased crushing of the beam concrete in Specimens C-P-Z4 and D-P-Z4 as observed during the tests.

An average increase of 30 percent ($\sigma = 22$ percent) in the energy dissipated per cycle was noted when prestressing strands (Specimens E-P-Z4 and F-P-Z4) were used in place of

post-tensioning bars (Specimens C-P-Z4 and D-P-Z4). As seen by the large standard deviations, the percent increase in energy dissipated per cycle was highly variable. The energy dissipated per cycle decreased by approximately 55 percent ($\sigma = 7$ percent) when partially bonded strands were used instead of fully bonded strands.

As shown in Fig. 25, the energy dissipated per cycle by precast Specimens E-P-Z4 and F-P-Z4 was an average of approximately 60 percent of that dissipated by the monolithic Zone 4 specimens. Also, the cyclic energy dissipated by Specimens G-P-Z4 and

H-P-Z4 was less than the cyclic energy dissipated by the monolithic Zones 2 and 4 specimens. This is due to the narrow and pinched hysteresis loops for these specimens.

The cumulative energy dissipated to failure by all the specimens is shown in Fig. 26. With respect to cumulative energy dissipated, the precast Zone 4 Specimens C through F performed better than the monolithic Zone 4 specimens. This was a result of the higher displacement ductilities achieved by these precast concrete specimens, which meant that these specimens underwent more reversed

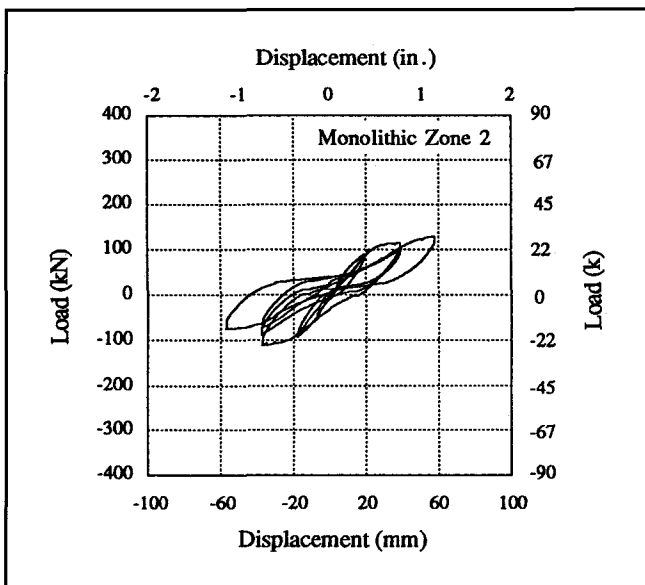


Fig. 21. Hysteresis plot for Specimen A-M-Z2.

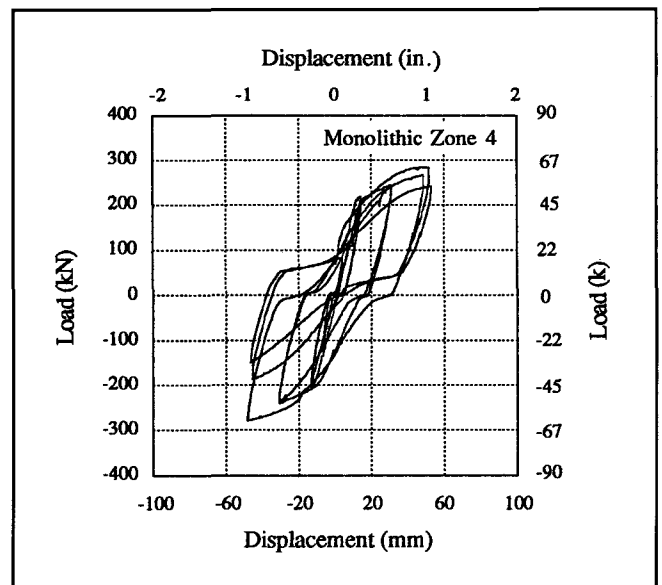


Fig. 22. Hysteresis plot for Specimen A-M-Z4.



Fig. 23. Representative failure mode for the precast concrete specimens.

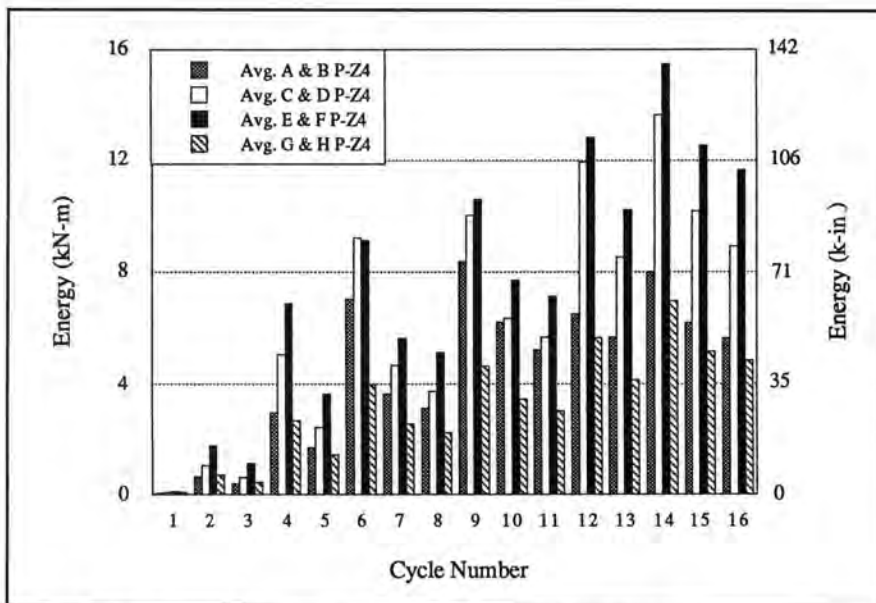


Fig. 24. Cyclic energy dissipated by precast Zone 4 specimens.

cyclic loading prior to failure.

The cumulative energy dissipated to failure by Specimens G-P-Z4 and H-P-Z4 was approximately equal to that for monolithic Zone 4 specimens. However, these specimens had not failed when the tests were stopped. Therefore, the cumulative energy dissipated by Specimens G-P-Z4 and H-P-Z4 as shown in Fig. 26 are minimum values.

Reinforcing Bar Yield

The yield lengths of the beam reinforcement give an indication of the strain concentration in the beam and,

therefore, an indication of the concentration of the beam rotation. The yield length of the reinforcement was measured from the column face. This length was obtained by first plotting the strain in the reinforcing bar against the distance of the strain gauge from the column face. The points were then connected with straight lines. The yield lengths were defined as the lengths from the column face to the point at which these lines crossed the nominal yield strain level.

As expected, the monolithic specimens exhibited longer reinforcing bar yield lengths than did the precast

specimens. This is due to the concentration of the rotation at the column face for the precast concrete specimens. The recorded strains in ties for the precast Zone 4 specimens were also much lower than for the monolithic specimens. Among the precast specimens, the specimens post-tensioned with bars had longer reinforcing bar yield lengths than those post-tensioned with strands. It would appear that the strains and rotations were more concentrated at the column joint for the specimens post-tensioned with strands.

CONCLUSIONS

1. Failure Mode — Failure modes for all precast concrete specimens were similar. Failure was characterized by yielding of the post-tensioning steel, beam crushing, and an opening at the junction between the beam and the column. The width of the opening at the beam-to-column joint increased as the post-tensioning steel was placed closer to the beam centroid. The width of the opening does not appear to be influenced by the type of post-tensioning steel (post-tensioning bars or prestressing strands) used to connect the precast concrete elements or by the use of partially debonded prestressing. It should be noted, however, that the partially bonded specimens were not tested to failure.

Unlike the monolithic Zone 2 specimens which failed predominantly in shear in the column joint region, the precast Zone 2 specimens did not experience severe joint distress.

2. Displacement Ductility — The ultimate displacement ductility for both precast Zone 2 specimens, $\mu_u = 4$, was lower than that obtained for the monolithic Zone 2 specimens, $\mu_u = 6$, and as a result, the precast concrete specimens had lower story drifts at failure.

In general, the precast concrete specimens had higher story drifts at failure and higher initial stiffnesses than the monolithic specimens. The ultimate displacement ductilities of the precast specimens ($\mu_u = 12$ and 14) were greater than those of the monolithic Zone 4 specimens, ($\mu_u = 6$). The experimental value of 14 for the par-

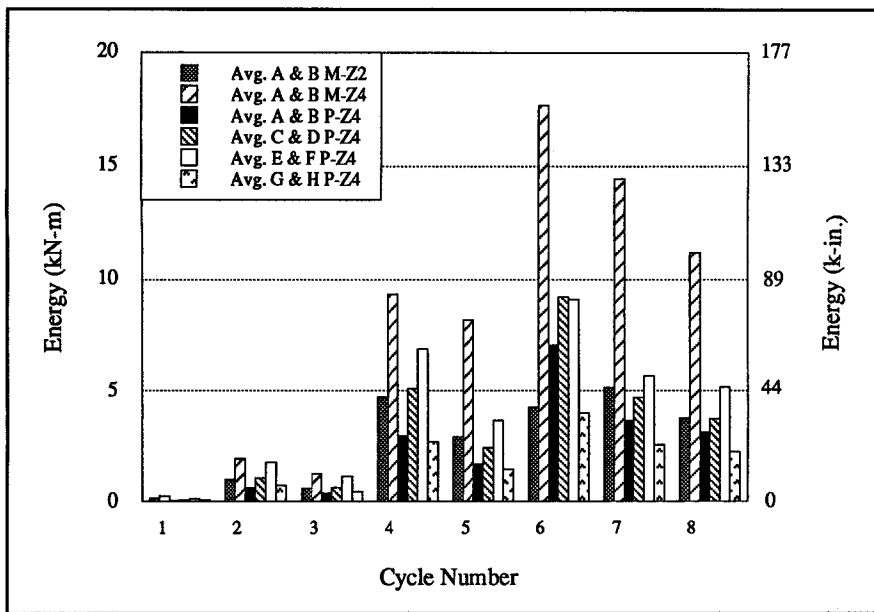


Fig. 25. Comparison of energy dissipated per cycle to $6\Delta_y$ (Cycle 3).

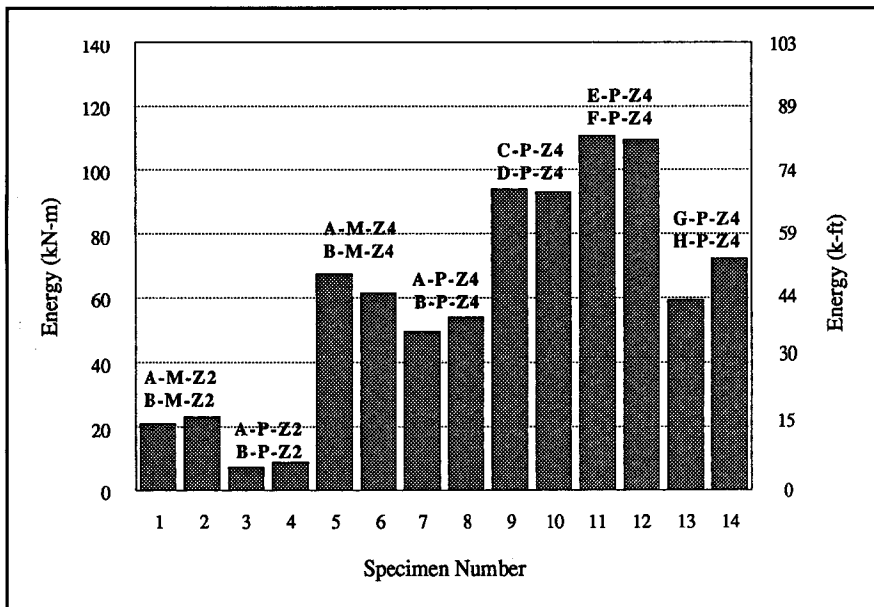


Fig. 26. Comparison of the cumulative energy dissipated to failure. Note: Specimens G-P-Z4 and H-P-Z4 had not failed when testing was stopped.

tially bonded specimens compared well with the predicted value of 15.6 by Priestley and Tao.⁸

3. Connection Strength — The measured maximum connection strengths for all the precast concrete specimens exceeded the calculated values and the precast specimens performed as well as the monolithic specimens in most cases. Based on the results obtained thus far, the experimental maximum moments for the precast specimens post-tensioned with strands were approximately 30 percent greater than the predicted mo-

ments. Placement of the post-tensioning bars closer to the beam centroid does not appear to have a significant adverse effect on the connection strength.

4. Energy Dissipation — As in Phase I, the energy dissipated per cycle by the precast Zone 4 specimens was less than that of the monolithic specimens. Energy dissipation per cycle improved from the use of prestressing strands instead of post-tensioning bars with the post-tensioning steel located closer to the beam centroid, and fully bonded. The energy

dissipated per cycle by Specimens E-P-Z4 and F-P-Z4 (the precast specimens which performed best with respect to energy dissipated per cycle) was, on the average, approximately 60 percent of that for the monolithic Zone 4 specimens.

In general, the cumulative energy dissipated to failure by precast Zone 4 specimens was greater than the cumulative energy dissipated by the monolithic Zone 4 specimens. This is due to the higher displacement ductilities achieved by the precast concrete specimens.

RECOMMENDATIONS

Test results obtained thus far show that a post-tensioned, precast beam-to-column connection appears to be a viable system for regions of high seismic activity. The shear friction between a precast beam and column has been shown to be sufficient to resist the applied shear loads without the need for corbels or shear keys. This type of post-tensioned precast concrete connection has also behaved as well as, and in most cases, better than similar monolithic connections in terms of connection strength and ductility.

In regions where energy dissipation is not an issue, the partially bonded specimens would be an attractive alternative as they have been shown to perform in what is essentially an elastic manner. Also, the amount of spiral steel used in the beam, with a volumetric ratio of 2 percent and a maximum pitch of $D/4$, was sufficient to confine the beam in the plastic hinge region.

FUTURE RESEARCH NEEDS

The precast concrete connections exhibited low energy dissipation per cycle as compared with monolithic connections. Phase IV of the test program will examine the use of low strength (mild) reinforcing steel in conjunction with post-tensioning as a means of improving the cyclic energy dissipation characteristics of the precast concrete specimens. The premise for this concept is that the mild steel will be used as an energy dissipator while the friction between the beam and the column caused by the post-

tensioning force will be used to provide the necessary shear resistance.

To address the concern that the previous NIST tests did not have gravity loads superimposed on the beams, simulated gravity loads will be applied to the beams of the Phase IV specimens. Other parameters that require further study are the amount of post-tensioning steel and mild reinforcing steel, the use of different concrete strengths and joint materials in the construction joint, and the influence of slabs and transverse beams on connection behavior.

ACKNOWLEDGMENT

The authors would like to express their gratitude to the individuals who contributed to this project. The assistance and support of the laboratory staff for the Building and Fire Research Laboratory, Structures Division, especially that of Frank Rankin, is gratefully acknowledged.

In addition, the technical guidance provided by the steering committee is

greatly appreciated. Members of the steering committee are Robert E. Englekirk, S. K. Ghosh, Daniel P. Jenny, (L. S.) Paul Johal and M. J. Nigel Priestley. The authors would also like to thank Suzanne D. Nakaki for providing the design of the test specimens.

REFERENCES

1. *Uniform Building Code*, International Conference of Building Officials, Whittier, CA, 1985.
2. Cheok, G. S., and Lew, H. S., "Performance of 1/4-Scale Model Precast Concrete Beam-Column Connections Subjected to Cyclic Inelastic Loads — Report No. 1," NISTIR 4433, National Institute of Standards and Technology, Gaithersburg, MD, October 1990.
3. Cheok, G. S., and Lew, H. S., "Performance of 1/4-Scale Model Precast Concrete Beam-Column Connections Subjected to Cyclic Inelastic Loads — Report No. 2," NISTIR 4589, National Institute of Standards and Technology, Gaithersburg, MD, June 1991.
4. Cheok, Geraldine S., and Lew, H. S., "Performance of Precast Concrete Beam-to-Column Connections Subject to Cyclic Loading," *PCI JOURNAL*, V. 36, No. 3, May-June 1991, pp. 56-67.
5. Bhatt, Prabhakara, and Kirk, D. W., "Tests on an Improved Beam Column Connection for Precast Concrete," *ACI Journal*, Proceedings, V. 82, No. 6, November-December 1985, pp. 834-843.
6. Bull, D. K., and Park, Robert, "Seismic Resistance of Frames Incorporating Precast Prestressed Concrete Beam Shells," *PCI JOURNAL*, V. 31, No. 4, July-August 1986, pp. 54-93.
7. French, Catherine, et al., "Connections Between Precast Elements — Failure Within Connection Region," *ASCE Structural Journal*, V. 114, No. 2, February 1989, pp. 3171-3192.
8. Priestley, M. J. Nigel, and Tao, Jian Ren, "Seismic Response of Precast Prestressed Concrete Frames With Partially Debonded Tendons," *PCI JOURNAL*, V. 38, No. 1, January-February 1993, pp. 58-69.
9. ACI Committee 318, "Building Code Requirements for Reinforced Concrete and Commentary (ACI 318-89)," American Concrete Institute, Detroit, MI, 1989.